Extended phase diagram of the three-dimensional phase field crystal model

2010 J. Phys.: Condens. Matter 22 205402

(http://iopscience.iop.org/0953-8984/22/20/205402)

J. Phys.: Condens. Matter **22** (2010) 205402 (4pp) doi:10.1088/0953-8984/22/20/205402

Extended phase diagram of the three-dimensional phase field crystal model

A Jaatinen[1,2] **and T Ala-Nissila**[1]

[1] Department of Applied Physics, Aalto University School of Science and Technology, PO Box 11000, FI-00076 Aalto, Finland
[2] Department of Materials Science and Engineering, Aalto University School of Science and Technology, PO Box 16200, FI-00076 Aalto, Finland

E-mail: Akusti.Jaatinen@tkk.fi

Received 21 January 2010, in final form 1 April 2010
Published 30 April 2010
Online at stacks.iop.org/JPhysCM/22/205402

Abstract
We determine the phase diagram of the phase field crystal model in three dimensions by using numerical free energy minimization methods. Previously published results, based on single mode approximations, have indicated that in addition to the uniform (liquid) phase, there would be regions of stability of body-centered cubic, hexagonal and stripe phases. We find that in addition to these, there are also regions of stability of face-centered cubic and hexagonal close packed structures in this model.

1. Introduction

One of the challenges in modern computational materials science is being able to access phenomena that take place on different time and length scales. Recently, a new model called the phase field crystal (PFC) model has been constructed that describes phenomena taking place on an atomic length scale but diffusive timescales [1, 2] the combination of which remains inaccessible for molecular dynamics (MD) simulations using present day computers. The PFC method is able to achieve this combination of scales by replacing the individual atoms in MD simulations by a continuous field that exhibits the periodic nature of the underlying atomic lattice in the solid phase, but evolves in diffusive timescales [3]. At present, the PFC model has already proven itself useful in modeling various phenomena, including elastic and plastic deformation of materials [2, 4], dislocation dynamics [5], crystal growth [6, 7] and the effect of an external force on two-dimensional layers [8–10]. However, being only a few years old, the methodology is still facing many topical challenges, including e.g. establishing a solid connection between the PFC model and more microscopic theories, as well as finding a way to obtain the parameters of the model for a given material [7, 11–13]. One of the current challenges in PFC modeling is being able to model different close packed crystal structures. Because the well-known single mode approximations to the original PFC free energy functional have not shown stable close packed crystal structures, some ad hoc modifications to the free energy functional have been proposed [14, 15]. In the present work, we show that a more accurate calculation of the extended phase diagram of the original PFC model reveals that the three-dimensional (3D) close packed hexagonal and cubic structures are in fact stable in a certain parameter range of the model. This means that at a qualitative level, the original PFC model can well be used to study these crystal structures without any modifications, although to construct a more quantitative model for the close packed phases we believe such modifications are indeed necessary.

2. Model

In phase field crystal modeling, one models an order parameter field that has periodic ground states, and is driven towards its ground state through dissipative dynamics. Thus, the key ingredient in such theory is a dynamical equation that drives the order parameter field towards its ground state given by a minimum of a free energy functional. A minimum requirement for a free energy functional for PFC studies is that it should have, at least in some parameter range, a periodic ground state. We study the simplest known free energy functionals that fulfil these requirements. These models are described by a free

energy that contains local contributions up to the fourth order, and also gradient terms up to fourth order. This family of free energy functionals was adapted to PFC models from the work of hydrodynamic fluctuations by Swift and Hohenberg [16], and they are the most simple and widely used free energy functionals in PFC studies to date ([1] and references therein), although some higher order models have also been proposed recently [13, 15]. We consider here the free energy of the system described by an order parameter $\phi(\mathbf{r})$, which is given by

$$F[\phi(\mathbf{r})] = \int \mathrm{d}\mathbf{r} \left\{ \frac{\phi(\mathbf{r})}{2}[a + \lambda(q_0^2 + \nabla^2)^2]\phi(\mathbf{r}) - \frac{b}{3}\phi(\mathbf{r})^3 + \frac{g}{4}\phi(\mathbf{r})^4 \right\}, \quad (1)$$

where a, λ, q_0, b and g are phenomenological parameters. The third order term is not included in all of the studies, but in the following we show that whether one includes this term or not does not make a difference to the qualitative features of the model. To do this, we introduce in equation (1) a set of new variables,

$$\mathbf{x} = q_0\mathbf{r}; \quad (2)$$

$$\psi = \sqrt{\frac{g}{\lambda q_0^4}}\left(\phi - \frac{b}{3g}\right); \quad (3)$$

$$\epsilon = \frac{1}{\lambda q_0^4}\left(\frac{b^2}{3g} - a\right). \quad (4)$$

We then ignore all terms that are either constant or linearly proportional to the dimensionless order parameter field ψ, as they will not make a contribution in a conserved model, and we define a dimensionless free energy $\mathcal{F}$ as $g\lambda^{-2}q_0^{-5}$ times the original free energy without the constant and linear parts. We end up with

$$\mathcal{F}[\psi(\mathbf{x})] = \int \mathrm{d}\mathbf{x} \left\{ \frac{\psi(\mathbf{x})}{2}[-\epsilon + (1 + \nabla^2)^2]\psi(\mathbf{x}) + \frac{1}{4}\psi(\mathbf{x})^4 \right\}, \quad (5)$$

which is exactly the same free energy one gets from the free energy without the third order term (e.g. [12]). Thus this variable change shows that the phase behavior of all models defined by equation (1), even with all the five parameters included, can be examined completely by studying the two-dimensional space spanned by ϵ and the average value of ψ.

In general, ϵ is often considered to be a small parameter. From a mathematical point of view, it is easier to derive amplitude expansions to this model, if one can make the assumption that ϵ is small [12, 17]. Some attempts to relate the parameters of equation (1), and thus ϵ, to physical quantities of real materials exist in the literature. An analysis of elastic and surface properties by Wu and Karma suggests that for iron this parameter should be on the order of 0.1, supporting the hypothesis of small ϵ [12]. However, the exact parameters will depend on the material studied and for qualitative studies it might even be desirable to use parameters that are unrealistic in some perspectives, if using such parameters will have some other benefit. For these reasons, in the present work we will not restrict ourselves to only the limit where ϵ is small. Instead, we aim at a more complete assessment of the phase diagram, allowing ϵ to vary between 0 and 1.8.

3. Results

In order to calculate the phase diagram of the PFC model we have calculated the free energies of liquid, body-centered cubic (bcc), face-centered cubic (fcc), hexagonal close packed (hcp), simple cubic, rods and stripes phases as a function of $\bar{\psi}$, i.e. the average value of $\psi(\mathbf{x})$ for each parameter ϵ studied. For calculating the free energy at a given point on $\bar{\psi}$, ϵ space, we have initialized a system of the size of a single unit cell with the one-mode approximation representing the given lattice structure (appendix A), with periodic boundary conditions. Then, we have employed a numerical integration of the conserved equation of motion,

$$\frac{\partial\psi}{\partial t} = \nabla^2\frac{\delta\mathcal{F}}{\delta\psi}, \quad (6)$$

to find the actual density profile that minimizes the free energy, and the free energy. The numerical method utilized for integrating the equation of motion is based on a semi-implicit operator splitting [18], with the Laplace operator discretized in Fourier space as $\Delta_{\mathbf{k}} = -k^2$. In addition, we minimize the free energy with respect to the lattice spacing of the periodic phases. This is achieved by calculating the free energy of a given phase with three different lattice spacings in parallel. Based on these, we calculate the first and second derivatives of the free energy with respect to the lattice spacing, and we then employ a Newton–Raphson iteration to find the lattice spacing that minimizes the free energy of the given phase at the given point in the $(\bar{\psi}, \epsilon)$ space. The spatial resolution used in this study is such that there are 16 grid points per unit cell in each direction. A small number of points in the phase diagram were checked with the spatial resolution doubled, and the results were found to be practically indistinguishable from the ones obtained using our standard resolution.

After calculating the minimum free energies of all the phases as a function of $\bar{\psi}$, the coexistence densities are found by using the standard common tangent construction, where the coexistence densities $\bar{\psi}_i$ and $\bar{\psi}_j$ of phases i and j are found through the relations

$$\left.\frac{\partial f_i(\bar{\psi}, \epsilon)}{\partial\bar{\psi}}\right|_{\bar{\psi}_i} = \left.\frac{\partial f_j(\bar{\psi}, \epsilon)}{\partial\bar{\psi}}\right|_{\bar{\psi}_j}; \quad (7)$$

$$f_j(\bar{\psi}_j, \epsilon) - f_i(\bar{\psi}_i, \epsilon) = \left.\frac{\partial f_i(\bar{\psi}, \epsilon)}{\partial\bar{\psi}}\right|_{\bar{\psi}_i}(\bar{\psi}_j - \bar{\psi}_i), \quad (8)$$

where f_i and f_j are the free energy densities of phases i and j, respectively. Equation (7) implies that at coexistence, the coexisting phases must have equal chemical potentials, and equation (8) implies that the pressures of the coexisting phase must also be equal.

From previous studies it is known that in the limit where ϵ is small, the one-mode approximations to the free energies of different phases become exact [2]. Results of our numerical calculations for the phase diagram in this limit are shown in figure 1, together with 'one-mode' results obtained by using our double tangent method with analytically derived one-mode approximations for the free energies of different phases

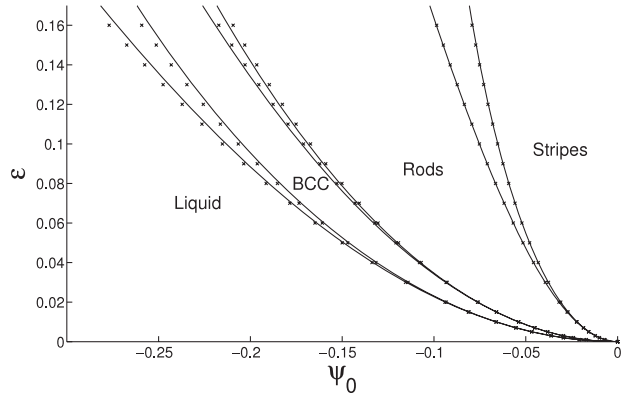

Figure 1. Small ϵ limit of the phase diagram. Crosses show points of coexistence as obtained from our numerical calculations and the lines show approximate results based on the single mode approximation.

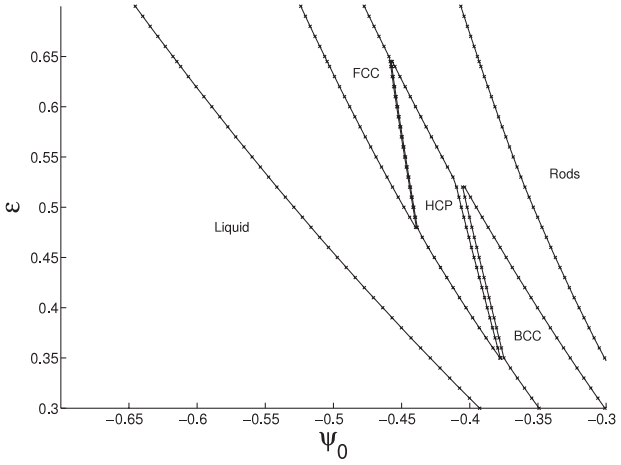

Figure 2. Part of the phase diagram where the hcp phase is stable. Symbols show the points obtained from our numerical calculations, with lines connecting the symbols.

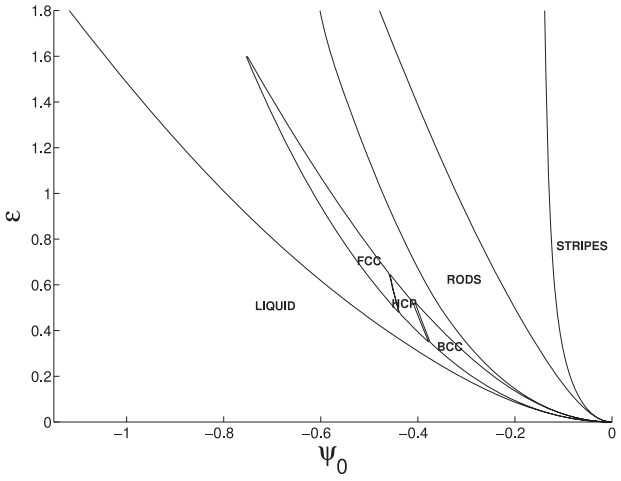

Figure 3. Phase diagram up to $\epsilon = 1.8$ as obtained from our numerical calculations. For clarity, the individual points where calculations were done are not shown.

(appendix A). Examining the results, we find very good agreement with the small ϵ analysis of Wu and Karma, which shows that the asymptotic behavior of liquid–bcc coexistence lines in the limit of small ϵ is given by $-\sqrt{45\epsilon/103}$, and the linear terms in their expansions as powers of $\epsilon^{1/2}$ are zero [12].

When ϵ is increased, the difference between one-mode and numerical results increases accordingly. This becomes exceedingly important for values of ϵ exceeding 0.35, because at that value, we find a triple coexistence of liquid, bcc and hcp structures. This result is in contradiction with the prediction from the one-mode approximation that the body-centered phase should always have a lower free energy than the close packed ones. Beyond that value, the liquid crystallizes into a stable hcp solid in the interval $\epsilon = 0.35 \cdots 0.48$. In the upper end of this interval, we find a triple coexistence, this time with liquid, hexagonal close packed and fcc phases coexisting with one another. From $\epsilon = 0.48$ upwards, the stable crystalline phase that forms from the liquid has a fcc structure.

The region of the phase diagram where all 3D crystalline phases are found, is shown in figure 2. It is seen that the coexistence gaps between the solid phases are very small, the difference in ψ_0 in the coexisting phases being on the order of 10^{-3} for bcc–hcp and 10^{-4} for hcp–fcc. Especially for the hcp–fcc boundary, a small difference in free energies, and thus a small coexistence gap, is expected due to the close resemblance of the two structures. Indeed, the differences in free energy densities of the two close packed phases in the relevant range is on the order of 10^{-5}, while the corresponding differences are on the order of 10^{-4} between bcc and close packed phases and 10^{-2} between crystalline and uniform phases. Due to the tiny differences in free energies of the fcc and hcp phases, reproducing the exact regimes of stability shown in figure 2 requires a numerical precision that is impractical for many numerical simulations. Therefore, the exact regimes of stability in a given simulation will, to some extent, depend on the numerical details of the method. We may also speculate that due to the tiny differences in free energies of the phases, including a Langevin noise in the equations of motion could alter the stability regimes even significantly, although the effect was not studied in the present work.

The stability regime of the fcc phase finally terminates in a triple coexistence with the rods phase at $\epsilon \approx 1.6$. Above that point, the stable phase that coexists with the uniform phase is the two-dimensional hexagonal structure. The total phase diagram up to $\epsilon = 1.8$ obtained from our numerical calculations is shown in figure 3.

The surprising result of finding regions where hcp and fcc phases are stable may be of great importance for modeling materials characterized by these structures with the PFC model. However, we have seen for the case of modeling metals with bcc structure that fitting the fourth order model studied with experimental material properties has limitations [13]. For the hcp and fcc phases, we see no reason to expect this situation to be better, especially as those phases stabilize even further away from the presumably physical limit where ϵ is small. In order to describe hcp and fcc materials quantitatively with

the PFC model, mathematical modifications to the free energy functional, such as very recently proposed by Wu *et al* [15], are very likely necessary. Despite that, it is presumably of interest to use this simple model for qualitative modeling of the various crystal structures.

4. Conclusion

We have determined the phase diagram of the Swift–Hohenberg phase field crystal model in three dimensions through numerical free energy minimization methods. As our most surprising finding, we find that there are regions of stability of fcc and hcp structures in this model. This means that at least on a qualitative level, the PFC model can be used to study phenomena in these phases without any modifications. However, we believe that in order to make the model reproduce selected physical properties of a given material, mathematical modifications of the free energy functional may be necessary.

Acknowledgments

This work has been supported in part by the Academy of Finland through its Center of Excellence COMP grant, Tekes through its MASIT33 project and EU Grant No. STRP 016447 MagDot.

Appendix A. Single mode approximations

Single mode approximations to the density profiles of different crystal structures are of the form

$$\psi(\mathbf{x}) = \bar{\psi} + A\varphi_i(\mathbf{x}), \tag{A.1}$$

where $\bar{\psi}$ is the mean value of $\psi(\mathbf{x})$, A_i is the amplitude of density fluctuations and $\varphi_i(\mathbf{x})$ is the single mode function obtained by summing, with equal weights, plane waves whose wavevectors constitute the principal set of reciprocal lattice vectors of the lattice in question. For the various phases studied, the φs are

$$\varphi_{\mathrm{BCC}}(\mathbf{x}) = \cos(qx)\cos(qy) + \cos(qx)\cos(qz) + \cos(qy)\cos(qz); \tag{A.2}$$

$$\varphi_{\mathrm{FCC}}(\mathbf{x}) = \cos(qx)\cos(qy)\cos(qz); \tag{A.3}$$

$$\varphi_{\mathrm{SC}}(\mathbf{x}) = \cos(qx) + \cos(qy) + \cos(qz); \tag{A.4}$$

$$\varphi_{\mathrm{Rods}}(\mathbf{x}) = \cos(qx)\cos\left(\frac{qy}{\sqrt{3}}\right) - \frac{1}{2}\cos\left(\frac{2qy}{\sqrt{3}}\right); \tag{A.5}$$

$$\varphi_{\mathrm{Stripes}}(\mathbf{x}) = \cos(qx), \tag{A.6}$$

where qs are inversely related to the lattice spacing. For the hexagonal close packed structure, there is no single mode function, thus we use the ansatz [6]

$$\begin{aligned}\varphi_{\mathrm{HCP}}(\mathbf{x}) = \Bigg[&\cos\left(\frac{2qy}{\sqrt{3}}\right) + \cos\left(qx - \frac{qy}{\sqrt{3}}\right) \\ &- \cos\left(\frac{2\pi}{3} - qx + \frac{qy}{\sqrt{3}}\right) + \cos\left(qx + \frac{qy}{\sqrt{3}}\right) \\ &- \cos\left(\frac{-4\pi}{3} + qx + \frac{qy}{\sqrt{3}}\right) \\ &- \cos\left(\frac{-2\pi + \sqrt{12}qy}{3}\right)\Bigg]\cos\left(\sqrt{\frac{3}{8}}qz\right).\end{aligned} \tag{A.7}$$

In order to find the single mode approximation to the free energy of a given phase as a function of its wavelength and amplitude, the density profile of that phase, defined by equation (A.1) and one of equations (A.2)–(A.7), is plugged in equation (5) and the integrals are evaluated analytically. Then the free energy is minimized w.r.t. A and q to find the approximate analytical expression to the free energy as a function of $\bar{\psi}$ and ϵ. Once these expressions are found for all the phases of interest, we solve numerically equations (7) and (8) to find the single mode approximations to the coexistence densities as a function of ϵ.

References

[1] Elder K R, Katakowski M, Haataja M and Grant M 2002 *Phys. Rev. Lett.* **88** 245701
[2] Elder K R and Grant M 2004 *Phys. Rev.* E **70** 051605
[3] Tupper P F and Grant M 2008 *Europhys. Lett.* **81** 40007
[4] Stefanovic P, Haataja M and Provatas N 2006 *Phys. Rev. Lett.* **96** 225504
[5] Berry J, Grant M and Elder K R 2006 *Phys. Rev.* E **73** 031609
[6] Tegze G, Granasy L, Toth G I, Podmaniczky F, Jaatinen A, Ala-Nissila T and Pusztai T 2009 *Phys. Rev. Lett.* **103** 035702
[7] van Teeffelen S, Backofen R, Voigt A and Lowen H 2009 *Phys. Rev.* E **79** 051404
[8] Achim C V, Karttunen M, Elder K R, Granato E, Ala-Nissila T and Ying S C 2006 *Phys. Rev.* E **74** 021104
[9] Achim C V, Karttunen M, Elder K R, Granato E, Ala-Nissila T and Ying S C 2008 *J. Phys.: Conf. Ser.* **100** 072001
[10] Achim C V, Ramos J A, Karttunen M, Elder K R, Granato E, Ala-Nissila T and Ying S C 2009 *Phys. Rev.* E **79** 011606
[11] Elder K R, Provatas N, Berry J, Stefanovic P and Grant M 2007 *Phys. Rev.* B **75** 064107
[12] Wu K-A and Karma A 2007 *Phys. Rev.* B **76** 184107
[13] Jaatinen A, Achim C V, Elder K R and Ala-Nissila T 2009 *Phys. Rev.* E **80** 031602
[14] Wu K-A 2006 Order-parameter models of microstructural evolution *PhD Thesis* Northeastern University
[15] Wu K-A, Adland A and Karma A 2010 arXiv:1001.1349v1
[16] Swift J and Hohenberg P C 1976 *Phys. Rev.* A **15** 319–28
[17] Goldenfeld N, Athreya B P and Dantzig J A 2005 *Phys. Rev.* E **72** 020601(R)
[18] Tegze G, Bansel G, Toth G I, Pusztai T, Fan Z and Granasy L 2009 *J. Comput. Phys.* **228** 1612–23